frontiers | Frontiers in Computational Neuroscience

TYPE Original Research
PUBLISHED 06 February 2026
DOI 10.3389/fncom.2026.1741793

Check for updates

OPEN ACCESS

EDITED BY
Tiago Ribeiro,
National Institutes of Health (NIH),
United States

REVIEWED BY
Silvia Scarpetta,
University of Salerno, Italy
Antonio Jorge Fontenele,
University of Arkansas, United States

*CORRESPONDENCE
Hardik Rajpal
✉ h.rajpal15@imperial.ac.uk

†These authors have contributed equally to this work

RECEIVED 07 November 2025
REVISED 12 January 2026
ACCEPTED 21 January 2026
PUBLISHED 06 February 2026

CITATION
Rajpal H, Stefens C, Saeedian M, Canzano JS, Kareithi MG, Barahona M, Smith SL, Schultz SR and Jensen HJ (2026) Synergy mediates long-range correlations in the visual cortex near criticality.
Front. Comput. Neurosci. 20:1741793.
doi: 10.3389/fncom.2026.1741793

COPYRIGHT
© 2026 Rajpal, Stefens, Saeedian, Canzano, Kareithi, Barahona, Smith, Schultz and Jensen. This is an open-access article distributed under the terms of the Creative Commons Attribution License (CC BY). The use, distribution or reproduction in other forums is permitted, provided the original author(s) and the copyright owner(s) are credited and that the original publication in this journal is cited, in accordance with accepted academic practice. No use, distribution or reproduction is permitted which does not comply with these terms.

Synergy mediates long-range correlations in the visual cortex near criticality

Hardik Rajpal[1,2,3]*, Cedric Stefens[4†], Meghdad Saeedian[1,2†], Joe S. Canzano[5†], Michael G. Kareithi[4], Mauricio Barahona[2], Spencer LaVere Smith[5], Simon R. Schultz[4] and Henrik Jeldtoft Jensen[1,2]

[1]Centre for Complexity Sciences, Imperial College London, London, United Kingdom, [2]Department of Mathematics, Imperial College London, London, United Kingdom, [3]I-X Centre for AI in Science, Imperial College London, London, United Kingdom, [4]Department of Bioengineering, Imperial College London, London, United Kingdom, [5]Department of Electrical and Computer Engineering, University of California, Santa Barbara, CA, United States

Long-range correlations are a key signature of systems operating near criticality, indicating spatially-extended interactions across large distances. These extended dependencies underlie other emergent properties of critical dynamics, such as high susceptibility and multi-scale coordination. In the brain, along with other signatures of criticality, long-range correlations have been observed across various spatial scales, suggesting that the brain may operate near a critical point to optimize information processing and adaptability. However, the mechanisms underlying these long-range correlations remain poorly understood. Here, we investigate the role of synergistic interactions in mediating long-range correlations in the visual cortex of awake mice. We leverage recent advances in mesoscale two-photon calcium imaging to analyse the activity of thousands of neurons across a wide field of view, allowing us to confirm the presence of long-range correlations at the level of neuronal populations. By applying the Partial Information Decomposition (PID) framework, we decompose the correlations into synergistic and redundant information interactions. Our results reveal that the increase in long-range correlations during visual stimulation is accompanied by a significant increase in synergistic rather than redundant interactions among neurons. Furthermore, we analyse a combined network formed by the union of synergistic and redundant interaction networks, and find that both types of interactions complement each other to facilitate efficient information processing across long distances. This complementarity is further enhanced during the visual stimulation. These findings provide new insights into the computational mechanisms that give rise to long-range correlations in neural systems and highlight the importance of considering different types of information interactions in understanding correlations in the brain.

KEYWORDS

calcium imaging, information, information decomposition, long-range interactions, multi-layer network, redundancy, synergy

1 Introduction

The theory of self-organized criticality (SOC) provides a framework for understanding how complexity arises in natural systems and a balance between order and disorder is maintained (Bak et al., 1988; Jensen, 1998). SOC suggests that complex systems naturally evolve toward a critical state, and, in such a state, small perturbations can lead to large-scale

events, often characterized by power-law distributions (Pruessner, 2012). This critical state exhibits enhanced information processing (Ito and Gunji, 1994; Birdsey et al., 2017; Munoz, 2018) and computational capabilities (Boedecker et al., 2012), as it allows for a balance between stability and adaptability (Ito and Gunji, 1994; Birdsey et al., 2017; Munoz, 2018). In addition, systems at criticality exhibit other desirable properties, such as maximal dynamic range (Kinouchi and Copelli, 2006) and long-range correlations across regions that can facilitate information integration (Jensen, 2021). These properties have inspired the *brain criticality hypothesis* (O'Byrne and Jerbi, 2022; Beggs and Timme, 2012; Shew and Plenz, 2013), which posits that the brain operates near a critical point to optimally process information, respond to a wide range of stimuli, and orchestrate a balance between functional segregation and integration (Hengen and Shew, 2025; Chialvo, 2010; Cocchi et al., 2017).

Empirical evidence supporting the brain criticality hypothesis has been observed across various spatial and temporal scales, from the microscopic level of individual neurons to the macroscopic level of large-scale brain networks. At the microscopic level, studies have reported that neuronal avalanches, which are cascades of neuronal firings separated by silence, follow power-law distributions, in accordance with the critical brain hypothesis (Beggs and Plenz, 2003; Shriki et al., 2013). At the macroscopic level, functional magnetic resonance imaging (fMRI) studies have shown that large-scale brain networks exhibit scale-free dynamics and long-range correlations, which are also suggestive of a critical state (Expert et al., 2010; Tagliazucchi et al., 2012).

More recently, studies have explored the role of criticality in cognitive processes, such as sensorimotor processing, perception, attention, and memory (Palva and Palva, 2018; Liu et al., 2025; Leisman and Koch, 2024; Iannello et al., 2025). Some studies have found that different signatures of brain criticality are sensitive to various states of consciousness, such as sleep, anesthesia, and disorders of consciousness (Tagliazucchi et al., 2016; Maschke et al., 2024; Zimmern, 2020). In computer science, it has been shown that artificial neural networks (ANNs) can benefit from operating near criticality, as it enhances generalization performance and enables learning of optimal representations (Bertschinger et al., 2004; Langton, 1990; Morales and Muñoz, 2021; Cramer et al., 2020). See recent reviews for a comprehensive overview of the state of research on brain criticality and its implications for brain dynamics in health and disease (Cocchi et al., 2017; Chialvo, 2010; O'Byrne and Jerbi, 2022; Beggs and Timme, 2012; Shew and Plenz, 2013; Wilting and Priesemann, 2019; Munoz, 2018; Hengen and Shew, 2025).

Despite the growing body of evidence supporting the brain criticality hypothesis, several challenges and open questions remain. Among the various signatures of criticality, the correlation length, which quantifies the spatial extent of neural correlations, is expected to diverge at criticality (Stanley, 1971). Functionally, the ensuing long-range correlations are crucial for facilitating coordination among various brain regions and information integration. While some work has been done to explore the presence of long-range correlations in macroscopic scales in fMRI studies (Expert et al., 2010), there is a need for experimental and computational studies to understand how long-range correlations manifest at the level of neuronal populations and how they relate to different cognitive states. So far, such studies have been limited to either *in-vitro* neuronal cultures or smaller populations of *in-vivo* neurons due to a lack of large-scale recordings.

Beyond identifying long-range correlations, it is also important to explore biological or computational mechanisms that give rise to spatially extended interactions. To address these questions, however, one needs to further decompose the nature of correlations in neural systems. Information theory provides a powerful framework to decompose the interdependencies between components of a system into different types, such as redundant, unique, and synergistic (Williams and Beer, 2010). Previous work explored how different types of information interactions emerge from stimulus-evoked vs. stimulus-independent correlations (Panzeri et al., 1999, 2022). Recent developments in information decomposition, such as the Partial Information Decomposition (PID) (Williams and Beer, 2010) and the Integrated Information Decomposition (Φ ID) (Mediano et al., 2025), have provided new tools to dissect the nature of correlations in neural systems. These approaches allow us to quantify the amount of redundant or synergistic information between different components of a system, as well as their unique contributions to a target variable or to the future state of the system. Synergistic interactions are particularly interesting, as they represent the information that is only available when considering multiple components together and cannot be obtained from any single component alone. For example, a post-synaptic neuron firing as an *XOR* gate of the inputs of the pre-synaptic neurons is a purely synergistic interaction, as the state of each pre-synaptic neuron alone does not provide any information about the state of the post-synaptic neuron (Mediano et al., 2025). Beyond neuroscience, synergy has been used to understand the different musical styles of Rosas et al. (2019); to differentiate the technological complexity of economies (Rajpal and Guerrero, 2025); and to study collective behavior of cells in organoids (Varley et al., 2025).

In this study, we leverage recent advances in mesoscale two-photon calcium imaging (Yu et al., 2021) that make it possible to record the activity of thousands of neurons across a wide field of view (up to several millimeters) of the visual cortex of awake mice. This allows us to explore the presence of long-range correlations and their relationship to criticality in neuronal populations. We then apply the PID framework to decompose the correlations into different types of information interactions and investigate how these interactions vary across different spatial scales. By combining large-scale *in-vivo* neuronal recordings with advanced information-theoretic analysis, we aim to provide computational insights into the mechanisms that give rise to long-range correlations. We also explore how these correlations and information interactions vary between spontaneous and visually stimulated states.

We find that the visual cortex exhibits long-range correlations that extend across several millimeters, and these correlations are enhanced under visual stimulation. By applying PID, we find that synergistic information interactions play a crucial role in mediating long-range correlations. Indeed, redundant interactions are dominant and have a longer correlation length; synergistic interactions exhibit a more pronounced increase at large distances during visual stimulation. We further analyse a combined network constructed from the synergistic and redundant interaction layers, and find that both synergistic and redundant interactions

complement each other to facilitate information processing across long distances. Our findings provide further support toward the brain criticality hypothesis by characterizing long-range correlations in the visual cortex. We show that long-range correlations are preferentially modulated by synergistic interactions among the neurons under visual stimulation. These results provide novel insights into the role of synergistic interactions in the brain to coordinate activity across brain regions and their relationship to the possible critical brain dynamics. Furthermore, it highlights the importance of considering different types of information interactions in understanding neural systems.

2 Materials and methods

The study is based on calcium imaging data recorded from the posterior cortex of awake mice using a two-photon mesoscope, including several visual areas. The datasets were preprocessed to extract the neural activity traces, which were then used for information-theoretic analyses. In this section, we describe the data acquisition, preprocessing steps, and the information-theoretic measures employed in our analysis.

2.1 Data acquisition

All experimental procedures were approved by the Institutional Animal Care and Use Committee (IACUC) at the University of California, Santa Barbara and were conducted in accordance with the guidelines of the US Department of Health and Human Services. The animals used in the study were adult, triple transgenic mice of the genotype TITL-GCaMP6s (Ai94, Madisen et al., 2015) X Emx1-Cre (Jackson Labs #005628) X ROSA:LNL:tTA (Jackson Labs #011008) to express the calcium indicator GCaMP6s in cortical excitatory neurons. The mice were housed in a 12-h reverse light/dark cycle and had *ad libitum* access to food and water. A total of 10 recordings (5 spontaneous and 5 stimulated) were obtained from 8 mice, with some mice contributing multiple recordings on different days. At least one week before experiments, mice were surgically implanted with a 5mm optical glass coverslip over the right posterior cortex and a stainless steel headplate, both adhered with cyanoacrylate glue (Oasis Medical) and dental cement (Parkell Metabond), as previously described (Schneider et al., 2025). After recovery, intrinsic signals optical imaging (**ISOI**) (Kalatsky and Stryker, 2003) was performed to measure cortical retinotopic maps used to delineate visual area boundaries, also as described previously (Yu et al., 2022; Smith et al., 2017). These were used to validate craniotomy targeting and to register the two-photon fields of view to visual areas via vascular landmarks.

The calcium imaging datasets were recorded at the University of California, Santa Barbara, using a custom-built two-photon mesoscope (Diesel2p) (Yu et al., 2021). The mesoscope allows for imaging large fields of view (herein, 3 mm × 3-4 mm) at resonant speeds and cellular resolution. The imaging was performed at a median frame rate of 7.5 Hz and 1.46 microns per pixel. Fields of view were positioned to cover primary visual cortex (V1) and several higher visual areas (HVAs) at once, at depths of 150–200 μm to capture L2/3 cortical neurons. Imaging sessions lasted approximately 45 minutes, during which the mice were either in a spontaneous state (no visual stimulus) or were presented with drifting grating patches as visual stimuli. The visual stimuli were presented on a 90 cm curved monitor placed 14.5 cm from the mouse's left eye and tilted 10 degrees downward to cover approximately 150 degrees of visual angle in azimuth and 70 degrees in elevation. Drifting grating patches were presented sequentially as 20-degree-wide squares tiling the visual field area above. Each had a spatial frequency of either 0.04 or 0.1 cpd and a temporal frequency of 1 or 4 Hz, and were presented in 8 different orientations (0, 45, 90, 135, 180, 225, 270, and 315 degrees). The parameters of the patches in each sequence were randomly shuffled across successive presentations to enforce an even stimulus distribution. Finally, a projective correction was applied to screen stimuli to account for the near placement of a flat screen and the spherical eye of the mouse (Smith, 2012); with the correction applied, images strictly maintain the intended geometry and location across the visual field relative to the eye center. Visible emission from the screen was blocked from the imaging objective using a custom opaque plastic cone placed between the headplate and objective. Spontaneous recordings were obtained in the absence of any visual stimuli, with the mice either in total darkness or with the same screen set to a static middle gray image. Further details of the recordings used in this study are provided in the Supplementary material.

2.2 Preprocessing

The raw calcium imaging data were first preprocessed using the Suite2p pipeline (Pachitariu et al., 2016), which includes motion correction and alignment using the registration module. The motion correction step in Suite2p involved aligning the frames of the imaging data to correct for any movement artifacts. The cell detection and extraction of the fluorescence traces were performed using the EXTRACT algorithm (Inan et al., 2017; Dinç et al., 2021), which identifies regions of interest (ROIs) corresponding to individual neurons and extracts their fluorescence signals, while correcting for any neuropil contamination. The extracted fluorescence traces were then deconvolved to estimate the underlying spiking rate using the deep-learning-based CASCADE algorithm (Rupprecht et al., 2021). Finally, to obtain the discretized binary states of each neuron, the deconvolved traces were fitted using a Hidden Markov Model (HMM) to identify the most probable state (Active: 1 or Quiet: 0) of each neuron at each time point (see Figure 1). This approach allows us to avoid setting an arbitrary threshold for each neuron and provides a probabilistic framework for identifying discrete states from the deconvolved calcium traces (Diana et al., 2019; Etter et al., 2020). The binarized states were then used for the correlation and information-theoretic analyses.

2.3 Information-theoretic measures

To measure the interdependencies between the neural activity traces recorded from the neurons in the visual cortex, we

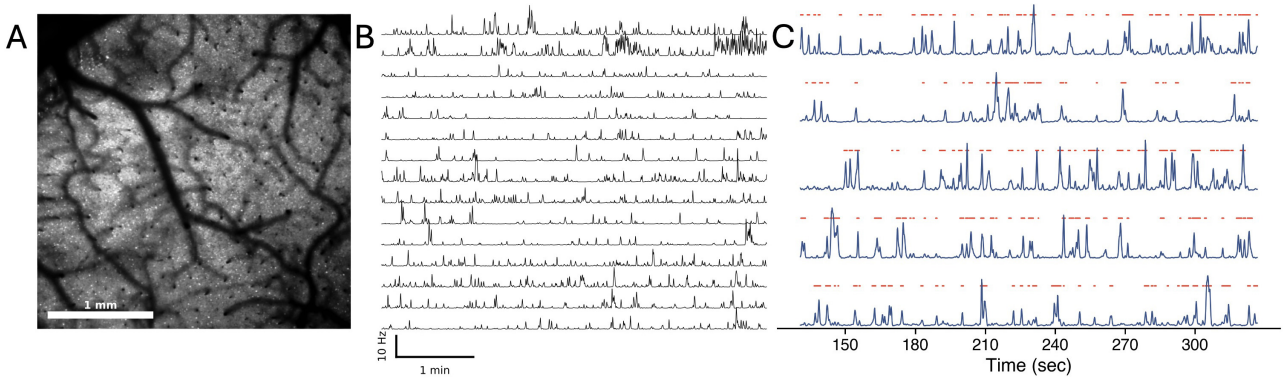

FIGURE 1
Data preprocessing pipeline. **(A)** Recorded field of view from the Diesel2p mesoscope. Neurons are visible as the bright spots in the image. **(B)** The deconvolved traces of spiking activity extracted from ROIs detected by the EXTRACT algorithm. **(C)** The binarized states used for subsequent analysis. The blue traces represent the spiking activity of individual neurons, and the red dots indicate the on states detected by the Hidden Markov Model (HMM).

build upon mutual information (MI). MI quantifies the mutual dependence between two variables by computing the amount of information obtained about one random variable through observing another random variable. For two discrete random vectors **U** and **V**, the mutual information of **U** given **V** is defined as:

$$I(\mathbf{U};\mathbf{V}) = \sum_{\mathbf{u}\in\mathcal{U}}\sum_{\mathbf{v}\in\mathcal{V}} p(\mathbf{u},\mathbf{v})\,\log\frac{p(\mathbf{u},\mathbf{v})}{p(\mathbf{u})\,p(\mathbf{v})}, \tag{1}$$

where $\mathbf{u}$ and $\mathbf{v}$ are values of the vector random variables **U** and **V**, respectively; $p(\mathbf{u},\mathbf{v})$ is the joint probability distribution function; and $p(\mathbf{u})$ and $p(\mathbf{v})$ are the marginal probability distribution functions.

Here, we compute the mutual information between binarized and deconvolved calcium traces. The HMM-based binarization helps to mitigate the effects of noise and variability in the calcium imaging data, and has been useful in the identification of neuronal assemblies (Diana et al., 2019) and decoding behavior (Etter et al., 2020).

2.3.1 Partial information decomposition

Let us consider two neurons X and Y, with observable states X_t and Y_t, respectively. To quantify the total information shared by this pair of neurons about their joint future activity after a time lag τ, we use the Time Delayed Mutual Information (TDMI), defined as $I(X_t, Y_t; X_{t+\tau}, Y_{t+\tau})$, where, according to the definition (Equation 1), we have $\mathbf{U} = [X_t, Y_t]$ given by the joint states of neurons X and Y at time t and $\mathbf{V} = [X_{t+\tau}, Y_{t+\tau}]$ by their joint states at a future time point $t+\tau$.

Using Partial Information Decomposition (PID) (Williams and Beer, 2010), we can decompose the TDMI into four non-negative components (see Figure 2): unique information from neuron X ($UI(X)$), unique information from neuron Y ($UI(Y)$), redundant information (RI), and synergistic information (SI). The decomposition is given by:

$$\begin{aligned} I(X_t, Y_t; X_{t+\tau}, Y_{t+\tau}) =& UI(X_t; X_{t+\tau}, Y_{t+\tau}) + UI(Y_t; X_{t+\tau}, Y_{t+\tau}) \\ &+ RI(X_t, Y_t; X_{t+\tau}, Y_{t+\tau}) \\ &+ SI(X_t, Y_t; X_{t+\tau}, Y_{t+\tau}) \end{aligned} \tag{2}$$

However, the PID framework does not provide a unique decomposition, as there are multiple ways to define the components. In this study, we employ the Minimum Mutual Information (MMI) approach to define the redundant information (Barrett, 2015) as:

$$\begin{aligned} RI(X_t, Y_t; X_{t+\tau}, Y_{t+\tau}) =& \min\{I(X_t; X_{t+\tau}, Y_{t+\tau}), \\ & I(Y_t; X_{t+\tau}, Y_{t+\tau})\} \end{aligned} \tag{3}$$

The MMI redundancy function provides an upper bound on the redundant information, but provides a non-negative and interpretable decomposition of the TDMI. The unique and synergistic information components can then be derived from the TDMI and the redundancy using the following equations:

$$\begin{aligned} UI(X_t; X_{t+\tau}, Y_{t+\tau}) &= I(X_t; X_{t+\tau}, Y_{t+\tau}) - RI(X_t, Y_t; X_{t+\tau}, Y_{t+\tau}) \\ UI(Y_t; X_{t+\tau}, Y_{t+\tau}) &= I(Y_t; X_{t+\tau}, Y_{t+\tau}) - RI(X_t, Y_t; X_{t+\tau}, Y_{t+\tau}) \\ SI(X_t, Y_t; X_{t+\tau}, Y_{t+\tau}) &= I(X_t, Y_t; X_{t+\tau}, Y_{t+\tau}) \\ &\quad - \max\{I(X_t; X_{t+\tau}, Y_{t+\tau}), I(Y_t; X_{t+\tau}, Y_{t+\tau})\} \end{aligned} \tag{4}$$

Here, $I(X_t; X_{t+\tau}, Y_{t+\tau})$ and $I(Y_t; X_{t+\tau}, Y_{t+\tau})$ are the mutual information between the past state of neuron X (or Y) and the joint future state of both neurons, $[X_{t+\tau}, Y_{t+\tau}]$. Note that, by the definition (Equation 3), one of the unique information components will be zero, depending on which neuron has the lower mutual information with the joint future state. In our analysis, we restrict ourselves to $\tau = 1$ as the time delay.

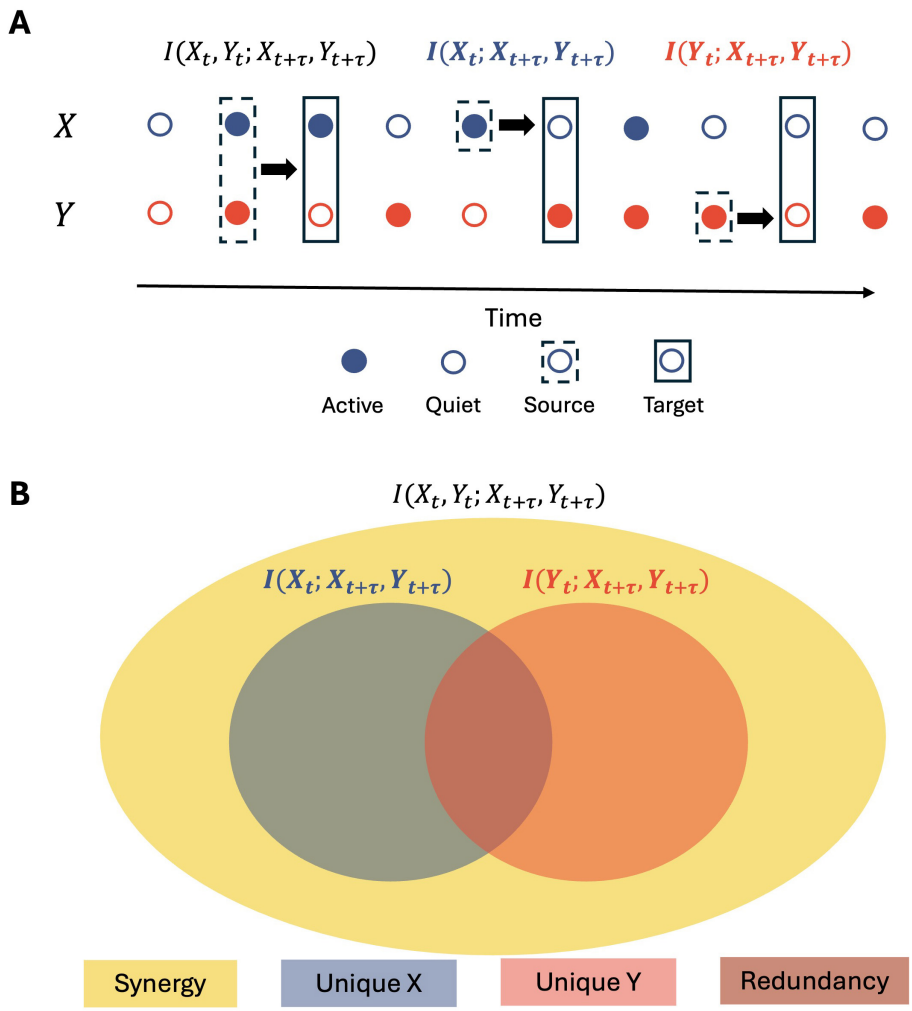

FIGURE 2
Partial information decomposition (PID) framework. **(A)** Schematic representation of two binary neurons X and Y, with their past states (X_t, Y_t) influencing their future states ($X_{t+\tau}$, $Y_{t+\tau}$) at a time lag τ. **(B)** The TDMI between the past states of neurons X and Y (X_t, Y_t) and their joint future states ($X_{t+\tau}$, $Y_{t+\tau}$) can be decomposed into four non-negative components: unique information from neuron X ($UI(X)$), unique information from neuron Y ($UI(Y)$), redundant information (RI), and synergistic information (SI).

2.3.2 Null models for information-theoretic measures

Our study involves the comparison of information-theoretic measures both within a dataset (across different recording paths) and across different datasets. Therefore, it is crucial to normalize these measures to account for potential biases arising from finite data size, firing rates, redundancy functions, and other confounding factors. To address this, we employ a null model-based normalization approach called NuMIT (Null Models for Information-Theoretic Measures) (Liardi et al., 2024).

NuMIT provides a systematic way to normalize the decomposed PID components by comparing them to null models that exhibit the same TDMI as the experimental data. The null models are generated by simulating a pair of neurons using randomly sampled binary processes constrained by adding independent noise to match the experimental TDMI. This ensures that the null models capture the same level of overall information transfer as the empirical data, while allowing us to assess the significance of the individual PID components. The normalization is performed by calculating the Z-scores of the empirical PID components relative to the null distributions. We can thus identify which components are significantly different from the expected value of the null models, constrained so that the overall time delayed information is preserved. The NuMIT framework has been shown to mitigate biases in information-theoretic measures and to accurately assess the underlying information dynamics in neural systems (Liardi et al., 2024).

2.4 Correlation length

To quantify the correlation length in the neural activity, we compute the pairwise Pearson correlation coefficient between the binarized spiking activity of all pairs of neurons in each dataset. The correlation coefficients are binned according to the inter-neuron distance, and the average correlation coefficient is then computed

for each of the logarithmically spaced distance bins. The correlation length λ is then estimated by fitting an exponential decay of the average correlation coefficient with distance:

$$C(d) = C_\infty + (C_0 - C_\infty)\, e^{-d/\lambda}. \tag{5}$$

Here, $C(d)$ is the average correlation coefficient at distance d, C_0 is the initial correlation coefficient at the minimum distance, C_∞ is the asymptotic correlation coefficient at large distances, which accounts for the baseline correlation in mesoscale calcium imaging data at large distances. The correlation length λ provides a characteristic length scale for the decay of correlations in space. The parameters, C_0, C_∞ and λ in Equation 5 were estimated by a non-linear least squares fitting algorithm using the *SciPy* library in Python (Virtanen et al., 2020). To visualize the decay of correlations with distance, we also defined the normalized average correlation coefficient:

$$C_{\text{norm}}(d) = \frac{C(d) - C_\infty}{C_0 - C_\infty} = e^{-d/\lambda}, \tag{6}$$

which allows for consistent comparison of the decay of correlations across different datasets and conditions.

The Z-scored Synergy and Redundancy values decay slowly with distance, with fitted λ beyond the field of view. To obtain more robust estimates of the spatial extent of information decay in the neural activity, we estimate the *effective information length* λ_{eff} as the normalized area under the curve of the fitted exponential decay function:

$$\lambda_{\text{eff}} = \frac{1}{C_0} \int_{d_0}^{d_{max}} C(d)\, \mathrm{d}d \tag{7}$$

where $d_0 = 100\mu m$ is the minimum distance and $d_{max} = 1500\mu m$ is the maximum distance in the field of view such that sufficient pairs of neurons are available.

2.5 Partial network decomposition

Within each dataset, we compute the pairwise synergistic and redundant interactions between neurons based on the normalized PID components. We formalize these interactions as networks, where the nodes are neurons and the edge weights correspond to the normalized synergistic (or redundant) information between the neurons. We then obtain the associated k-nearest neighbor (kNN) graph, whereby we retain only the top k strongest connections for each neuron. This results in a sparsified network representation that highlights the most relevant interactions while reducing noise and spurious connections.

To carry out our analysis using partial network decomposition, we consider the two unweighted networks (synergistic and redundant) and a *combined network* that contains the union of the edge sets from the synergistic and redundant layers (see Figure 3). This combined representation allows us to analyse the interplay between synergistic and redundant interactions and their contributions to the overall information propagation in the neural system. Using partial network decomposition (Luppi et al., 2024), we identify complementary, shared, and unique shortest paths between pairs of neurons across the synergistic and redundant layers (see Figure 3). This analysis provides insights into how the different types of information interactions contribute to the overall connectivity and information flow in the network across different spatial scales.

Briefly, the framework considers shortest paths between pairs of nodes as a measure of efficiency. Suppose we have a combined network with two layers, A and B, representing synergistic and redundant interactions, respectively. For each pair of nodes (i, j), we identify the shortest paths in each layer separately, denoted as $d_A(i, j)$ and $d_B(i, j)$. We then consider the shortest path on the combined network, which includes the union of the edges from both layers, and we denote it as $d_{A\cup B}(i, j)$. The partial network decomposition then classifies the shortest paths into three categories:

- **Complementary paths**: $d_{A\cup B}(i, j) < \min(d_A(i, j), d_B(i, j))$. This indicates that the interaction between the two layers provides a more efficient route for information transfer than either layer alone.
- **Shared paths**: $d_{A\cup B}(i, j) = \max(d_A(i, j), d_B(i, j))$. This indicates that the interaction between the two layers does not provide any additional efficiency for information transfer beyond what is already available in either layer.
- **Unique paths**: $d_{A\cup B}(i, j) = \min(d_A(i, j), d_B(i, j))$ and $d_{A\cup B}(i, j) < \max(d_A(i, j), d_B(i, j))$. This indicates that one layer provides a more efficient route for information transfer than the other layer, and the interaction between the two layers does not provide any additional efficiency.

By analyzing the distribution of complementary, shared, and unique paths, we can characterize how the contribution of synergistic and redundant interactions varies over paths of different lengths in the network.

3 Results

3.1 Long-range correlations in the visual cortex

We first investigate the presence of long-range correlations in the neural activity recorded from the visual cortex of awake mice. In Figure 4A (left), we plot the average Pearson correlation coefficients between the binarized spiking activity of two neurons as a function of the distance between the neurons (binned), for both spontaneous and visually stimulated conditions. The results show that the average correlations decay with distance, but remain significantly above zero even at distances of several millimeters, indicating the presence of long-range correlations in the neural activity. In Supplementary Materials, we show how the shape of the correlation distribution changes with distance. The fitted correlation functions (Equation 5) are also shown in Figure 4A (left). From each fit, we obtain values for the initial correlation C_0, correlation length λ and asymptotic correlation C_∞. The normalized correlations (Equation 6) shown in Figure 4A (right) highlight the increased correlation length observed during visual stimulation. Figure 4B shows that the initial correlation C_0 is not significantly different (Mean difference $= 0.002$, $p = 0.0871$ and Hedge's $g = 0.91$) among the datasets in the two conditions,

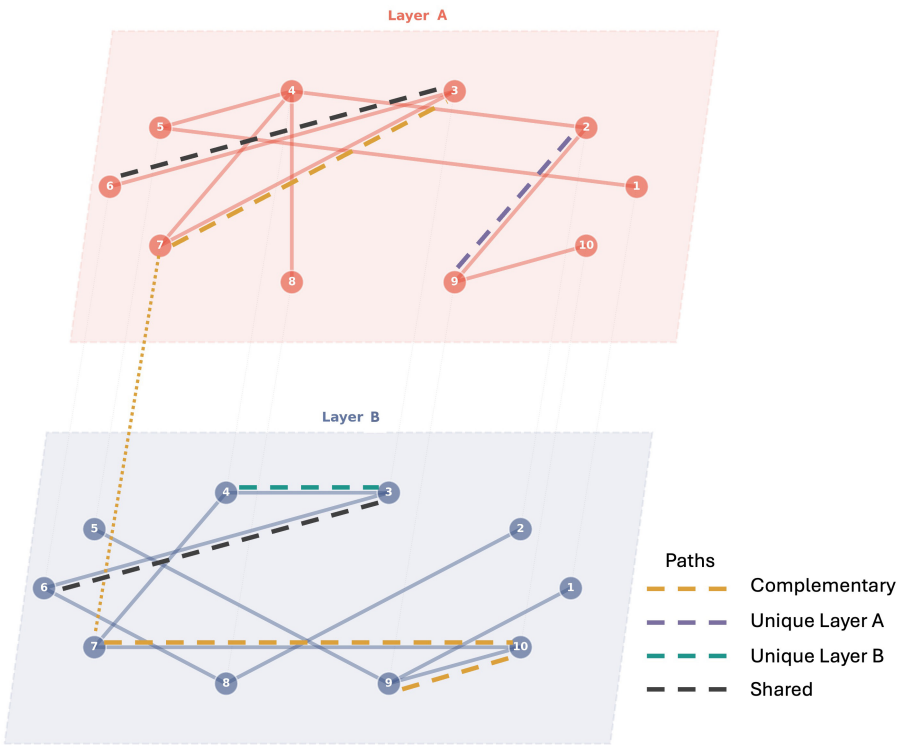

FIGURE 3
Partial network decomposition. Schematic representation of a combined network formed by Layers A and B. The different types of shortest paths between the nodes are illustrated using dashed lines: Complementary Paths (orange), Shared Paths (black), and Unique Paths (purple and teal). For instance, the shortest path between nodes 3 and 9 is complementary (orange), as it leverages connections from both layers to achieve a shorter path than either layer alone. The edge between nodes 3 and 6 is present in both layers, representing a shared path (black). The shortest path between nodes 2 and 9 is unique to Layer A (purple), while the shortest path between nodes 3 and 4 is unique to Layer B (teal).

yet the estimated correlation lengths are significantly larger (Mean difference $= 603.21\mu m$, $p = 0.0055$ and Hedge's $g = 2.25$) during visual stimulation compared to spontaneous activity, suggesting that visual input enhances long-range correlations in the visual cortex. An increased correlation length is a signature of a system operating closer to criticality (Stanley, 1971). It must be noted that although an increase in correlations is expected due to the visual stimulus for short distances ($\approx 200-300\mu m$) (Marshel et al., 2011), we observe increased correlations up to $\approx 900\mu m$. This indicates a distinct state of the cortical network that supports longer-range correlations rather than short-range stimulus-related co-activations. However, other factors, such as changes in attentional states or arousal levels during visual stimulation, may also contribute to the observed increase in correlation length (Vinck et al., 2015). Therefore, further investigation is needed to fully understand the biological mechanisms that modulate these long-range correlations. Furthermore, we observe that the fitted correlation functions fit the data well for large distances, but tend to overestimate correlations at short distances (see Figure 4A). This may be due to the presence of local heterogeneities and anti-correlations among the neurons in the field of view (between $100-200\mu m$), which are not captured by the exponential decay model. Future work could explore more complex correlation functions to better capture the full range of correlation behaviors observed in the data.

3.2 Information decomposition reveals distinct spatial profiles of synergy and redundancy

Next, we apply PID and NuMIT to decompose the time-delayed mutual information (TDMI) between pairs of neurons into Z-scored redundant and synergistic components. The TDMI was estimated at a time delay of $\tau = 1$ time step. The average Z-scored synergy and redundancy as a function of distance between pairs of neurons are shown in Figure 5. Both redundancy (Figure 5A, left) and synergy (Figure 5B, left) exhibit a decay with distance, but average initial redundancy (Z-score = 1.24 ± 0.06) is generally higher than synergy (Z-score = 0.23 ± 0.021), and the decay is slower for redundancy ($\lambda_{\text{eff}} = 1278 \pm 11\mu m$) compared to synergy ($\lambda_{\text{eff}} = 1230 \pm 41\mu m$). This suggests that redundant information is more prevalent and more spatially extended in the visual cortex. These findings are consistent with previous studies that have reported that sensory regions of the brain exhibit high levels of redundancy, which may serve to enhance the robustness and reliability of sensory processing (Luppi et al., 2022). The normalized Z-score plots on the right highlight the distinct spatial profiles of synergy and redundancy in the two contexts (see Figure 5A, B, right). While the spatial decay of redundancy is similar in both spontaneous and visually stimulated conditions, synergy exhibits a slower decay during visual stimulation compared

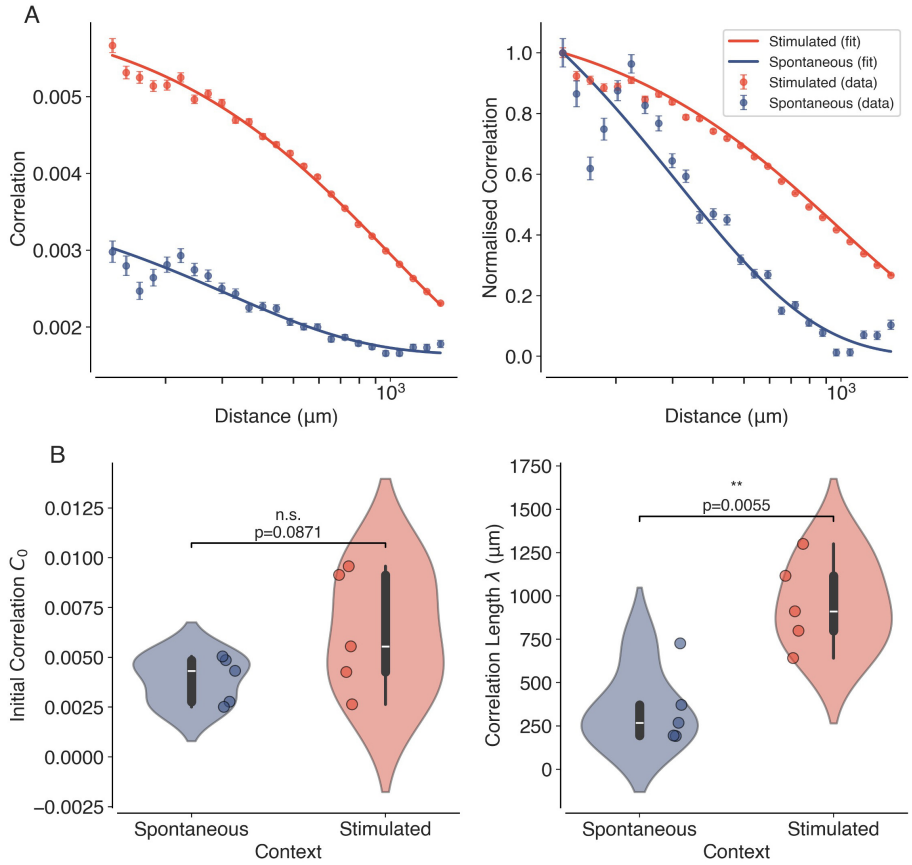

FIGURE 4
Long-range correlations in the visual cortex. **(A)** Average Pearson correlation coefficients (left) as a function of distance between pairs of neurons, for both spontaneous (blue) and visually stimulated (orange) conditions. The normalized correlation coefficients are shown on the right. The solid lines represent the fitted exponential decay functions. The error bars show the standard error of the mean. The slower decay of correlations in the stimulated condition is clearly visible in the normalized plots. **(B)** Violin plots showing the estimated correlation lengths λ for spontaneous and visually stimulated conditions across all datasets. Individual data points ($N = 10$, 5 Spontaneous and 5 Stimulated) are overlaid as dots. Asterisks indicate statistical significance (**, $p < 0.01$), estimated using permutation tests.

to spontaneous activity. This indicates the enhanced role of synergistic interactions in supporting long-range correlations during visual processing.

The fits also allow us to obtain *effective information lengths* for synergy and redundancy across all datasets, as shown in Figure 5C. We observe that while the redundancy information lengths do not significantly change (Mean difference $= 8.33\mu m$, $p = 0.150$ and Hedge's $g = 0.61$) between spontaneous and stimulated datasets, the synergy information lengths are significantly larger (Mean difference $= 56.67\mu m$, $p = 0.023$ and Hedge's $g = 1.08$) during visual stimulation compared to spontaneous activity. This suggests that visual stimulation enhances the spatial extent of synergistic interactions in the visual cortex, which may facilitate more efficient information processing and integration across different regions, whereas stimulation has little effect on the spatial extent of redundant interactions. Overall, these results highlight the unique role of synergistic interactions in mediating the increase of the spatial extent of long-range correlations, a signature of criticality.

3.3 Partial network decomposition reveals complementary roles of synergy and redundancy networks

To further investigate the interplay between synergistic and redundant interactions in the visual cortex, we apply partial network decomposition to combined networks, where neurons are nodes and the unweighted edges of the sparsified redundancy and synergy layers are constructed from the corresponding normalized components.

We then compute the complementary, shared, and unique paths that contribute to the propagation of information in the combined network representing the neurons of the visual cortex and their different interactions.

The proportion of complementary, shared, and unique paths as a function of path length is shown for both the spontaneous and stimulated conditions in Figure 6. We observe that the proportion of complementary paths increases with path

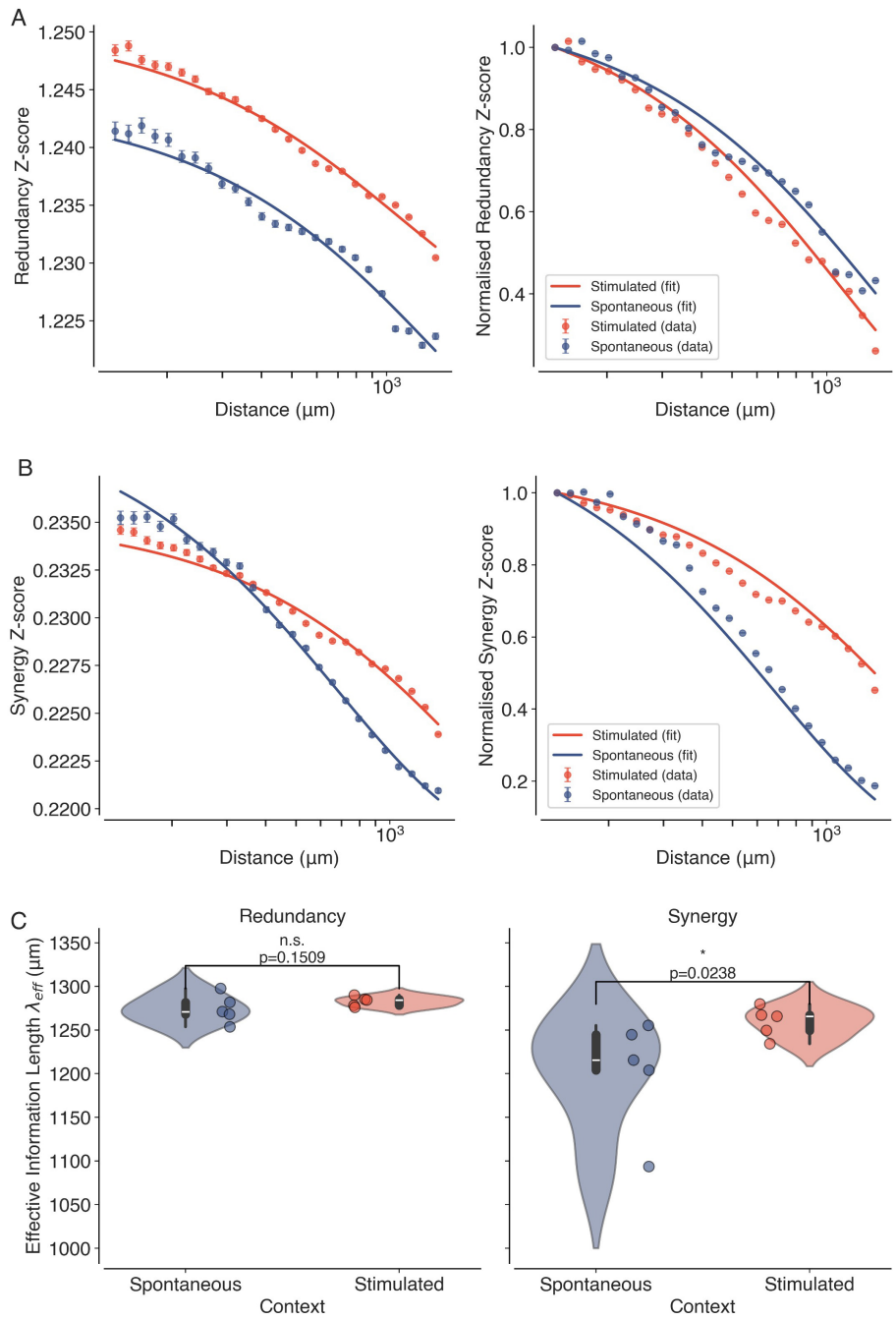

FIGURE 5
Information decomposition reveals distinct spatial profiles of synergy and redundancy. **(A)** Average and Normalised Z-scored Redundancy and **(B)** Synergy values as a function of distance between pairs of neurons, for both spontaneous (blue) and visually stimulated (orange) conditions. The solid lines represent the fitted exponential decay functions (Equation 5). The error bars show the standard error of the means. **(C)** Violin plots showing the estimated effective correlation lengths λ_{eff} for synergy and redundancy across all datasets ($N = 10$, 5 Spontaneous, and 5 Stimulated) in spontaneous (blue) and visually stimulated conditions (orange). Individual data points are overlaid as dots. Asterisk indicates statistical significance (*, $p < 0.05$), estimated using permutation tests.

length, indicating that synergistic and redundant interactions work together to facilitate efficient information processing across longer distances. The proportion of unique paths decreases with path length, and there are very few shared paths across all path lengths. These findings suggest that synergistic and redundant interactions complement each other over longer paths while maintaining a unique presence over shorter paths.

During stimulation, we observe a significant increase in the proportion of long (path length ≥ 4) complementary paths (Mean difference $= 0.105$, $p = 0.0008$) and a decrease in the proportion of long unique paths in the redundancy layer (Mean difference

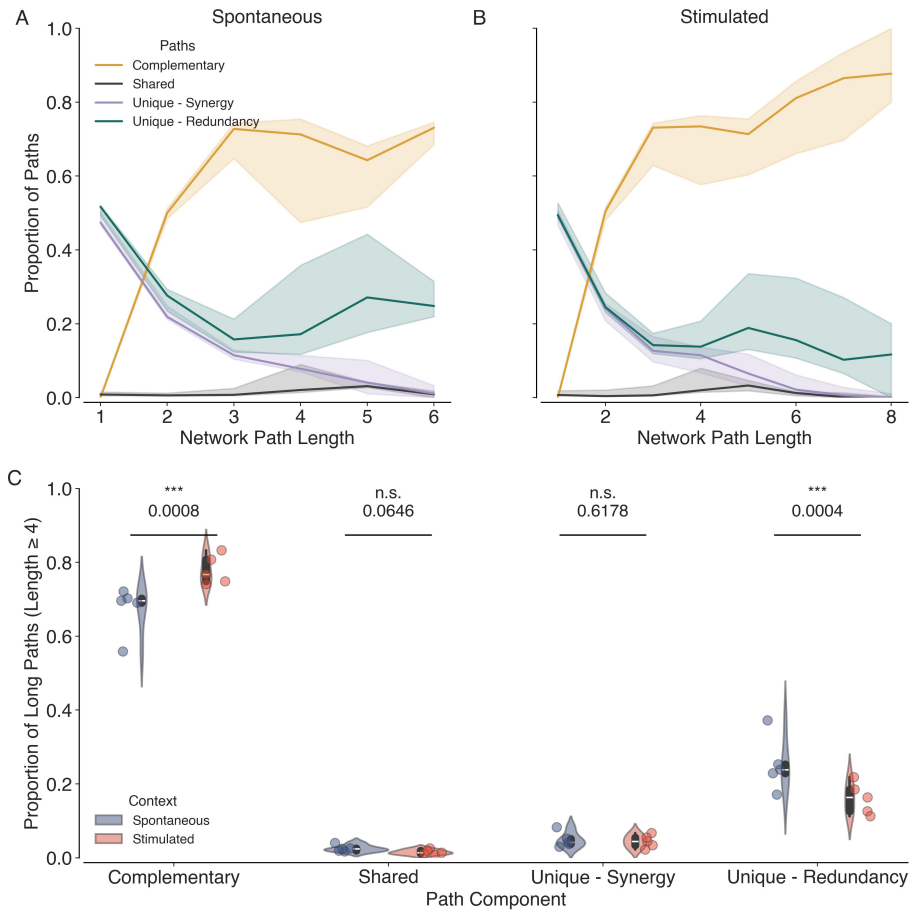

FIGURE 6
Partial network decomposition reveals complementary roles of synergy and redundancy networks. Proportion of complementary (orange), shared (black), and unique paths (purple and teal) as a function of network path length for both spontaneous **(A)** and stimulated **(B)** conditions. The solid lines represent the median across all datasets, and the shaded areas represent 95% confidence intervals. **(C)** Violin plots showing the proportion of long complementary, shared and unique paths among the synergy and redundancy layers across all datasets ($N = 10$, 5 Spontaneous, and 5 Stimulated) in spontaneous (blue) and stimulated conditions (orange). Individual data points are overlaid as dots. Asterisk indicates statistical significance (***, $p < 0.001$) estimated via permutation tests.

$= -0.09$, $p = 0.0005$), compared to spontaneous activity. This suggests that enhanced cooperative interactions between synergy and redundancy networks are observed at the expense of unique paths in the redundancy network during visual stimulation. These results highlight the dynamic nature of information interactions in the brain and their modulation by sensory input.

4 Discussion

In this study, we investigated the presence of long-range correlations in the neural activity recorded from the visual cortex of awake mice and explored the role of synergistic and redundant interactions in mediating these correlations. Using two-photon calcium imaging data from the mesoscope, we found that the visual cortex exhibits long-range correlations that are enhanced during visual stimulation. By applying the PID framework, we decomposed the time-delayed mutual information into synergistic and redundant components, and found that synergy plays a crucial role in mediating long-range correlations. Furthermore, the partial network decomposition revealed that both synergistic and redundant interactions cooperatively enable information processing over long distances in the visual cortex, especially under stimulation, when complementary paths become more important at the expense of unique redundant paths.

By identifying the presence of long-range correlations in the visual cortex, we provide support for the brain criticality hypothesis, which posits that the brain operates near a critical point to optimally process information and respond to a wide range of stimuli (O'Byrne and Jerbi, 2022; Beggs and Timme, 2012; Shew and Plenz, 2013). The dilated correlation lengths observed during visual stimulation suggest that sensory input can modulate the critical state of the brain, potentially allowing for more efficient information processing and integration across different regions. However, it must be noted that increased correlation lengths can arise due to increased arousal (Huo et al., 2024) or attention (Harris and Thiele, 2011), and not necessarily due to the visual stimulus itself. In future work, we are exploring the differential roles of arousal and stimulus in explaining the move toward criticality in the visual cortex.

We observe that redundant interactions are stronger and decay more slowly than synergistic interactions in the primary visual cortex. This finding is in line with the view of redundancy as a mechanism for enhancing the robustness of information processing (Luppi et al., 2022). On the other hand, synergistic interactions exhibit a more pronounced increase at large distances during visual stimulation, suggesting their unique role in coordinating spatially distributed information processing. We note that this selective enhancement of synergy departs from the increase in both synergy and redundancy near criticality in traditional models such as the Ising model (Marinazzo et al., 2019). This suggests that the brain may employ more complex mechanisms to regulate information interactions, beyond what is captured by simple models of criticality. Future studies could explore which biological mechanisms can explain the selective enhancement of synergy when approaching criticality in computational models of brain criticality.

Our work highlights the importance of considering different types of information interactions in understanding neural systems. Although this study focuses on time-delayed pairwise interactions, future studies could extend this framework to higher-order (beyond pairwise) interaction measures. Furthermore, although our focus has been on the primary visual cortex, it would be interesting to explore how these findings generalize to other brain regions and cognitive processes. The tools and frameworks presented here provide an approach to study the link between long-range correlations and information propagation mechanisms in neural systems, and could be applied to other datasets and experimental paradigms.

Data availability statement

The raw data supporting the conclusions of this article will be made available by the authors, without undue reservation.

Ethics statement

The animal study was approved by the Institutional Animal Care and Use Committee (IACUC) at the University of California, Santa Barbara. The study was conducted in accordance with the local legislation and institutional requirements.

Author contributions

HR: Writing – original draft, Methodology, Conceptualization, Visualization, Formal analysis, Validation, Writing – review & editing. CS: Writing – review & editing, Visualization, Data curation, Methodology. MS: Validation, Methodology, Formal analysis, Writing – review & editing. JC: Methodology, Investigation, Data curation, Writing – review & editing. MK: Data curation, Writing – review & editing. MB: Funding acquisition, Writing – review & editing, Project administration, Methodology, Supervision. SLS: Supervision, Writing – review & editing, Resources, Data curation. SRS: Funding acquisition, Project administration, Methodology, Writing – review & editing, Supervision. HJ: Project administration, Methodology, Supervision, Conceptualization, Writing – review & editing, Funding acquisition.

Funding

The author(s) declared that financial support was received for this work and/or its publication. HR, MS, CS, MB, SS, and HJ were supported by the Statistical Physics of Cognition project funded by the EPSRC (Grant No. EP/W024020/1). HR is also supported by the Eric and Wendy Schmidt AI in Science Postdoctoral Fellowship. JC and SLS were supported by NIH grants R01EY035378 and R01NS121919.

Acknowledgments

We thank the members of the Statistical Physics of Cognition project, Prof. Lucilla de Arcangelis, Dr. Pedro Mediano, Dr. Fernando Rosas, and Alberto Liardi for helpful discussions and feedback on the manuscript. We also thank the Imperial College High Performance Computing Service for computational resources.

Conflict of interest

The author(s) declared that this work was conducted in the absence of any commercial or financial relationships that could be construed as a potential conflict of interest.

Generative AI statement

The author(s) declared that generative AI was used in the creation of this manuscript. Language models were used for grammar correction and proofreading purposes only.

Any alternative text (alt text) provided alongside figures in this article has been generated by Frontiers with the support of artificial intelligence and reasonable efforts have been made to ensure accuracy, including review by the authors wherever possible. If you identify any issues, please contact us.

Publisher's note

All claims expressed in this article are solely those of the authors and do not necessarily represent those of their affiliated organizations, or those of the publisher, the editors and the reviewers. Any product that may be evaluated in this article, or claim that may be made by its manufacturer, is not guaranteed or endorsed by the publisher.

Supplementary material

The Supplementary Material for this article can be found online at: https://www.frontiersin.org/articles/10.3389/fncom.2026.1741793/full#supplementary-material

References

Bak, P., Tang, C., and Wiesenfeld, K. (1988). Self-organized criticality. *Phys. Rev. A* 38:364. doi: 10.1103/PhysRevA.38.364

Barrett, A. B. (2015). Exploration of synergistic and redundant information sharing in static and dynamical gaussian systems. *Phys. Rev. E* 91:052802. doi: 10.1103/PhysRevE.91.052802

Beggs, J. M., and Plenz, D. (2003). Neuronal avalanches in neocortical circuits. *J. Neurosci.* 23, 11167–11177. doi: 10.1523/JNEUROSCI.23-35-11167.2003

Beggs, J. M., and Timme, N. (2012). Being critical of criticality in the brain. *Front. Physiol.* 3:163. doi: 10.3389/fphys.2012.00163

Bertschinger, N., Natschläger, T., and Legenstein, R. (2004). "At the edge of chaos: real-time computations and self-organized criticality in recurrent neural networks," in *Advances in Neural Information Processing Systems*, 17.

Birdsey, L., Szabo, C., and Falkner, K. (2017). "Identifying self-organization and adaptability in complex adaptive systems," in *2017 IEEE 11th International Conference on Self-Adaptive and Self-Organizing Systems (SASO)* (IEEE), 131–140. doi: 10.1109/SASO.2017.22

Boedecker, J., Obst, O., Lizier, J. T., Mayer, N. M., and Asada, M. (2012). Information processing in echo state networks at the edge of chaos. *Theory Biosci.* 131, 205–213. doi: 10.1007/s12064-011-0146-8

Chialvo, D. R. (2010). Emergent complex neural dynamics. *Nat. Phys.* 6, 744–750. doi: 10.1038/nphys1803

Cocchi, L., Gollo, L. L., Zalesky, A., and Breakspear, M. (2017). Criticality in the brain: a synthesis of neurobiology, models and cognition. *Prog. Neurobiol.* 158, 132–152. doi: 10.1016/j.pneurobio.2017.07.002

Cramer, B., Stöckel, D., Kreft, M., Wibral, M., Schemmel, J., Meier, K., et al. (2020). Control of criticality and computation in spiking neuromorphic networks with plasticity. *Nat. Commun.* 11:2853. doi: 10.1038/s41467-020-16548-3

Diana, G., Sainsbury, T. T., and Meyer, M. P. (2019). Bayesian inference of neuronal assemblies. *PLoS Comput. Biol.* 15:e1007481. doi: 10.1371/journal.pcbi.1007481

Dinç, F., Inan, H., Hernandez, O., Schmuckermair, C., Hazon, O., Tasci, T., et al. (2021). Fast, scalable, and statistically robust cell extraction from large-scale neural calcium imaging datasets. *BioRxiv, 2021–03*. doi: 10.1101/2021.03.24.436279

Etter, G., Manseau, F., and Williams, S. (2020). A probabilistic framework for decoding behavior from *in vivo* calcium imaging data. *Front. Neural Circuits* 14:19. doi: 10.3389/fncir.2020.00019

Expert, P., Lambiotte, R., Chialvo, D. R., Christensen, K., Jensen, H. J., Sharp, D. J., et al. (2010). Self-similar correlation function in brain resting-state functional magnetic resonance imaging. *J. R. Soc. Interf.* 8, 472–479. doi: 10.1098/rsif.2010.0416

Harris, K. D., and Thiele, A. (2011). Cortical state and attention. *Nat. Rev. Neurosci.* 12, 509–523. doi: 10.1038/nrn3084

Hengen, K. B., and Shew, W. L. (2025). Is criticality a unified setpoint of brain function? *Neuron* 113, 2582–2598. doi: 10.1016/j.neuron.2025.05.020

Huo, C., Lombardi, F., Blanco-Centurion, C., Shiromani, P. J., and Ivanov, P. C. (2024). Role of the locus coeruleus arousal promoting neurons in maintaining brain criticality across the sleep-wake cycle. *J. Neurosci.* 44:e1939232024. doi: 10.1523/JNEUROSCI.1939-23.2024

Iannello, L., Tonelli, F., Cremisi, F., Calcagnile, L. M., Mannella, R., Amato, G., et al. (2025). Criticality in neural cultures: insights into memory and connectivity in entorhinal-hippocampal networks. *Chaos, Solit. Fractals* 194:116184. doi: 10.1016/j.chaos.2025.116184

Inan, H., Erdogdu, M. A., and Schnitzer, M. (2017). "Robust estimation of neural signals in calcium imaging," in *Advances in Neural Information Processing Systems*, 30.

Ito, K., and Gunji, Y.-P. (1994). Self-organisation of living systems towards criticality at the edge of chaos. *BioSystems* 33, 17–24. doi: 10.1016/0303-2647(94)90057-4

Jensen, H. J. (1998). *Self-Organized Criticality: Emergent Complex Behavior in Physical and Biological Systems*. Cambridge: Cambridge University Press. doi: 10.1017/CBO9780511622717

Jensen, H. J. (2021). What is critical about criticality: in praise of the correlation function. *J. Phys.* 2:032002. doi: 10.1088/2632-072X/ac24f2

Kalatsky, V. A., and Stryker, M. P. (2003). New paradigm for optical imaging: temporally encoded maps of intrinsic signal. *Neuron* 38, 529–545. doi: 10.1016/S0896-6273(03)00286-1

Kinouchi, O., and Copelli, M. (2006). Optimal dynamical range of excitable networks at criticality. *Nat. Phys.* 2, 348–351. doi: 10.1038/nphys289

Langton, C. G. (1990). Computation at the edge of chaos: Phase transitions and emergent computation. *Physica D* 42, 12–37. doi: 10.1016/0167-2789(90)90064-V

Leisman, G., and Koch, P. (2024). Resonating with the world: thinking critically about brain criticality in consciousness and cognition. *Information* 15:284. doi: 10.3390/info15050284

Liardi, A., Rosas, F. E., Carhart-Harris, R. L., Blackburne, G., Bor, D., and Mediano, P. A. (2024). Null models for comparing information decomposition across complex systems. *arXiv preprint arXiv:2410.11583*.

Liu, X., Fei, X., and Liu, J. (2025). The cognitive critical brain: modulation of criticality in perception-related cortical regions. *Neuroimage* 305:120964. doi: 10.1016/j.neuroimage.2024.120964

Luppi, A. I., Mediano, P. A., Rosas, F. E., Holland, N., Fryer, T. D., O'Brien, J. T., et al. (2022). A synergistic core for human brain evolution and cognition. *Nat. Neurosci.* 25, 771–782. doi: 10.1038/s41593-022-01070-0

Luppi, A. I., Olbrich, E., Finn, C., Suárez, L. E., Rosas, F. E., Mediano, P. A., et al. (2024). Quantifying synergy and redundancy between networks. *Cell Rep. Phys. Sci.* 5:101892. doi: 10.1016/j.xcrp.2024.101892

Madisen, L., Garner, A. R., Shimaoka, D., Chuong, A. S., Klapoetke, N. C., Li, L., et al. (2015). Transgenic mice for intersectional targeting of neural sensors and effectors with high specificity and performance. *Neuron* 85, 942–958. doi: 10.1016/j.neuron.2015.02.022

Marinazzo, D., Angelini, L., Pellicoro, M., and Stramaglia, S. (2019). Synergy as a warning sign of transitions: the case of the two-dimensional ising model. *Phys. Rev. E* 99:040101. doi: 10.1103/PhysRevE.99.040101

Marshel, J. H., Garrett, M. E., Nauhaus, I., and Callaway, E. M. (2011). Functional specialization of seven mouse visual cortical areas. *Neuron* 72, 1040–1054. doi: 10.1016/j.neuron.2011.12.004

Maschke, C., O'Byrne, J., Colombo, M. A., Boly, M., Gosseries, O., Laureys, S., et al. (2024). Critical dynamics in spontaneous eeg predict anesthetic-induced loss of consciousness and perturbational complexity. *Commun. Biol.* 7:946. doi: 10.1038/s42003-024-06613-8

Mediano, P. A., Rosas, F. E., Luppi, A. I., Carhart-Harris, R. L., Bor, D., Seth, A. K., et al. (2025). Toward a unified taxonomy of information dynamics via integrated information decomposition. *Proc. Nat. Acad. Sci.* 122:e2423297122. doi: 10.1073/pnas.2423297122

Morales, G. B., and Muñoz, M. A. (2021). Optimal input representation in neural systems at the edge of chaos. *Biology* 10:702. doi: 10.3390/biology10080702

Munoz, M. A. (2018). Colloquium: Criticality and dynamical scaling in living systems. *Rev. Mod. Phys.* 90:031001. doi: 10.1103/RevModPhys.90.031001

O'Byrne, J., and Jerbi, K. (2022). How critical is brain criticality? *Trends Neurosci.* 45, 820–837. doi: 10.1016/j.tins.2022.08.007

Pachitariu, M., Stringer, C., Schröder, S., Dipoppa, M., Rossi, L. F., Carandini, M., et al. (2016). Suite2p: beyond 10,000 neurons with standard two-photon microscopy. *BioRxiv, 061507*. doi: 10.1101/061507

Palva, S., and Palva, J. M. (2018). Roles of brain criticality and multiscale oscillations in temporal predictions for sensorimotor processing. *Trends Neurosci.* 41, 729–743. doi: 10.1016/j.tins.2018.08.008

Panzeri, S., Moroni, M., Safaai, H., and Harvey, C. D. (2022). The structures and functions of correlations in neural population codes. *Nat. Rev. Neurosci.* 23, 551–567. doi: 10.1038/s41583-022-00606-4

Panzeri, S., Schultz, S. R., Treves, A., and Rolls, E. T. (1999). Correlations and the encoding of information in the nervous system. *Proc. R. Soc. London Series B* 266, 1001–1012. doi: 10.1098/rspb.1999.0736

Pruessner, G. (2012). *Self-Organised Criticality: Theory, Models and Characterisation*. Cambridge: Cambridge University Press. doi: 10.1017/CBO9780511977671

Rajpal, H., and Guerrero, O. (2025). Synergistic small worlds that drive technological sophistication. *PNAS Nexus* 4:pgaf102. doi: 10.1093/pnasnexus/pgaf102

Rosas, F. E., Mediano, P. A., Gastpar, M., and Jensen, H. J. (2019). Quantifying high-order interdependencies via multivariate extensions of the mutual information. *Phys. Rev. E* 100:032305. doi: 10.1103/PhysRevE.100.032305

Rupprecht, P., Carta, S., Hoffmann, A., Echizen, M., Blot, A., Kwan, A. C., et al. (2021). A database and deep learning toolbox for noise-optimized, generalized spike inference from calcium imaging. *Nat. Neurosci.* 24, 1324–1337. doi: 10.1038/s41593-021-00895-5

Schneider, M., Canzano, J., Peng, J., Hou, Y., Smith, S. L., and Beyeler, M. (2025). Mouse vs. AI: a neuroethological benchmark for visual robustness and neural alignment. *ArXiv, arXiv-2509*.

Shew, W. L., and Plenz, D. (2013). The functional benefits of criticality in the cortex. *Neurosci.* 19, 88–100. doi: 10.1177/1073858412445487

Shriki, O., Alstott, J., Carver, F., Holroyd, T., Henson, R. N., Smith, M. L., et al. (2013). Neuronal avalanches in the resting MEG of the human brain. *J. Neurosci*. 33, 7079–7090. doi: 10.1523/JNEUROSCI.4286-12.2013

Smith, I. T., Townsend, L. B., Huh, R., Zhu, H., and Smith, S. L. (2017). Stream-dependent development of higher visual cortical areas. *Nat. Neurosci*. 20, 200–208. doi: 10.1038/nn.4469

Smith, S. L. (2012) *Visual Stimuli for Mice*. Labrigger. Available online at: http://labrigger.com/blog/2012/03/06/mouse-visual-stim/

Stanley, H. E. (1971). *Phase Transitions and Critical Phenomena*. Oxford: Clarendon Press.

Tagliazucchi, E., Balenzuela, P., Fraiman, D., and Chialvo, D. R. (2012). Criticality in large-scale brain fmri dynamics unveiled by a novel point process analysis. *Front. Physiol*. 3:15. doi: 10.3389/fphys.2012.00015

Tagliazucchi, E., Chialvo, D. R., Siniatchkin, M., Amico, E., Brichant, J.-F., Bonhomme, V., et al. (2016). Large-scale signatures of unconsciousness are consistent with a departure from critical dynamics. *J. R. Soc. Interf*. 13:20151027. doi: 10.1098/rsif.2015.1027

Varley, T. F., Pai, V. P., Grasso, C., Lunshof, J., Levin, M., and Bongard, J. (2025). Identification of brain-like complex information architectures in embryonic tissue of xenopus laevis organoids. *Commun. Integr. Biol*. 18:2568307. doi: 10.1080/19420889.2025.2568307

Vinck, M., Batista-Brito, R., Knoblich, U., and Cardin, J. A. (2015). Arousal and locomotion make distinct contributions to cortical activity patterns and visual encoding. *Neuron* 86, 740–754. doi: 10.1016/j.neuron.2015.03.028

Virtanen, P., Gommers, R., Oliphant, T. E., Haberland, M., Reddy, T., Cournapeau, D., et al. (2020). Scipy 1.0: fundamental algorithms for scientific computing in python. *Nat. Methods* 17, 261–272. doi: 10.1038/s41592-019-0686-2

Williams, P. L., and Beer, R. D. (2010). Nonnegative decomposition of multivariate information. *arXiv preprint arXiv:1004.2515*.

Wilting, J., and Priesemann, V. (2019). 25 years of criticality in neuroscience—established results, open controversies, novel concepts. *Curr. Opin. Neurobiol*. 58, 105–111. doi: 10.1016/j.conb.2019.08.002

Yu, C.-H., Stirman, J. N., Yu, Y., Hira, R., and Smith, S. L. (2021). Diesel2p mesoscope with dual independent scan engines for flexible capture of dynamics in distributed neural circuitry. *Nat. Commun*. 12:6639. doi: 10.1038/s41467-021-26736-4

Yu, Y., Stirman, J. N., Dorsett, C. R., and Smith, S. L. (2022). Selective representations of texture and motion in mouse higher visual areas. *Curr. Biol*. 32, 2810–2820.e5. doi: 10.1016/j.cub.2022.04.091

Zimmern, V. (2020). Why brain criticality is clinically relevant: a scoping review. *Front. Neural Circuits* 14:54. doi: 10.3389/fncir.2020.00054